Electrochemical Assembly and Potential-Dependent Plasmon Absorption of Au Nanoclusters Covered with a 4-Aminothiophenol Self-Assembled Monolayer

Masayuki Okamura, Toshihiro Kondo,‡ and Kohei Uosaki*

Physical Chemistry Laboratory, Division of Chemistry, Graduate School of Science, Hokkaido University, Sapporo 060-0810, Japan

Received: October 19, 2004; In Final Form: March 29, 2005

Gold nanoclusters covered with 4-aminothiophenol (4-ATP) self-assembled monolayers (SAMs) were electrochemically assembled on an Au or ITO electrode. The assembly mechanism is discussed on the basis of results of electrochemical, FT-IR, and XPS measurements. The intensity of plasmon absorption of the gold nanocluster assembly was shown to be dependent on applied potential as a result of electrochemical doping/undoping of a counteranion in the polyaniline film.

Introduction

Nanometer-sized metal nanoclusters possess interesting optical, electronic, chemical, and electrochemical properties, which are different from those of bulk materials, including surface plasmon absorption. Since the report by Brust et al.,[1] gold nanoclusters (GNCs) covered by self-assembled monolayers (SAMs) of alkanethiols have attracted the attention of many research groups[2−17] because SAM-covered GNCs are highly stable and can be prepared relatively easily. GNCs with special functionalities can be constructed by using thiol molecules with special functional groups, utilizing the rich references on alkanethiol SAMs with various functionalities.[18−27]

One of the most interesting properties of metal nanoclusters is plasmon absorption, and it is important to find a way to control the intensity and wavelength of surface plasmon absorption both for fundamental science and practical application.[28−31] Many theoretical formulas such as Mie's equation[32] have been proposal to describe the plasmon absorption of metal nanoclusters.[33] The absorption coefficient (α) of a metal nanocluster, which is smaller than about 20 nm, is given by[34]

$$\alpha = \frac{18\pi}{\ln 10}\frac{10^5}{\lambda}\frac{M{n_0}^3}{\rho}\frac{\epsilon_2}{(\epsilon_1 + 2{n_0}^2)^2 + {\epsilon_2}^2} \qquad (1)$$

where λ is the wavelength of light in nm, M and ρ are the molecular weight and density of the metal, respectively, n_0 is the refractive index of the medium, and ϵ_1 and ϵ_2 are real and imaginary components of the dielectric constant of bulk metal (ϵ: $\epsilon = \epsilon_1 + i\epsilon_2$), respectively. Thus, intensity of plasmon absorption depends on the refractive index of the medium. In other words, the intensity of plasmon absorption of metal nanoclusters can be controlled by controlling the refractive index of the medium.

Structurally controlled growth of mono- and multilayers of metal and semiconductor nanoclusters on solid surfaces has been attempted with the aim of construction of novel materials with various interesting characteristics of nanoclusters. Several techniques, including self-assembly,[35−41] electrostatic interaction between an anion and a cation,[9,10,42−48] the Langmuir−Blodgett method,[49−51] and electrochemical oxidation of a functional group of SAM on metal nanoclusters[14,16,17,52−54] have been employed to construct such multilayers.

Conducting polymers have attracted the attention of many research groups due to their interesting properties and wide variety of applications. The color and conductivity of conducting polymers depend on the potential as a result of electrochemical doping/undoping of a counteranion in the films.[55,56] Their applications include sensors,[57−61] cathode material of a lithium secondary battery,[62−69] and microelectronic devices.[70]

Conductive polymers with dispersed metal nanoclusters should exhibit interesting properties reflecting the properties of these two materials. Dispersion of GNCs within a conductive polymer has already been attempted by reducing $HAuCl_4$.[71] It is, however, more useful if SAM-modified size-controlled GNCs can be incorporated in a conductive polymer in a controlled manner. It is also expected that plasmon absorption intensity can be controlled by applied potential, and the properties of the film should be strongly dependent on the oxidation states of the films.

In this study, we demonstrated that GNC modified with 4-aminothiophenol (4-ATP) SAM can be assembled electrochemically through electrochemical polymerization of the aniline moiety of the SAM and that the intensity of plasmon absorption of the GNC assembly can be controlled by electrode potential as a result of electrochemical doping/undoping of a counteranion in the polyaniline film.

Experimental Section

Materials. $HAuCl_4$ (99.99%), $NaBH_4$ (practical grade), ethanol (superpure grade), hexanethiol (C_6SH, pure grade) and $HClO_4$ (superpure grade) were purchased from Wako Pure Chemicals. Tetra-*n*-octylammonium bromide (extra pure grade) and 4-aminothiophenol (4-ATP, >96%) were purchased from Tokyo Kasei Kogyo. Toluene (spectroscopic grade) was obtained from Dojindo Laboratory. All chemicals were used as received. Ultrapure water was obtained using a Milli-Q water purification system (Millipore), and ultrapure N_2 gas (99.999%) was obtained from Air Water. ITO-coated glass was obtained

* Author to whom correspondence should be addressed. Tel.: +81-11-706-3812. Fax.: +81-11-706-3440. E-mail: Uosaki@pcl.sci.hokudai.ac.jp.
‡ Present address: Department of Chemistry, Faculty of Science, Ochanomizu University, Bunkyo-ku, Tokyo 112-8610, Japan.

10.1021/jp045236u CCC: $30.25
Published on Web 05/03/2005

SCHEME 1: Preparation of 4-ATP-Modified Au Nanocluster

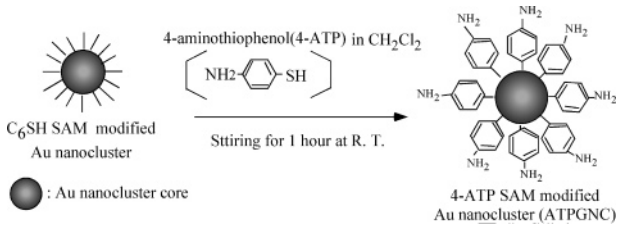

from Kinotone (resistivity: 8.3−9.8 Ω cm^{-2}). Gold disk (ϕ = 8 mm) was obtained from Tanaka Precious Metals.

Preparation of SAM-Protected Au Nanoclusters. C_6SH SAM-modified Au nanocluster (H-GNC) was prepared by the method reported by Brust et al.[1] Briefly, 100 mL of 20 mM $HAuCl_4$ aqueous solution was mixed with 300 mL of 30 mM tetra-*n*-octylammonium bromide toluene solution. The two-phase mixture was vigorously stirred until all of the $HAuCl_4$ had been transferred to the organic layer, that is, the color of the organic phase had changed to dark orange. Then, 0.68 g of C_6SH (5.8 mmol) was added to the organic phase. After stirring the mixture for 10 min, 100 mL of a freshly prepared 260 mM $NaBH_4$ aqueous solution was slowly added with vigorous stirring. After further vigorous stirring of the mixture for 3 h, the organic phase was extracted with dichloromethane. The volume of the organic residue was reduced to 10 mL in a rotary evaporator, and then 400 mL of ethanol was added to remove the excess C_6SH. After the mixture had been kept overnight at −18 °C, the dark-brown precipitate was filtered off and washed with ethanol. The crude product was dissolved in 10 mL of toluene and precipitated again by adding 400 mL of ethanol. The formation of H-GNC was confirmed by ^1H NMR (JEOL, JNM-EX 270 NMR, 270 MHZ). The core size of the H-GNC was determined by transmission electron microscopy (TEM, JEOL-2000EX, 200 kV) as approximately 1.8 nm.

C_6SH SAM of the H-GNC surface was replaced by 4-ATP by the place-exchange method (Scheme 1).[8] 4-ATP (0.08 g) was added to the H-GNC (0.2 g) dispersion in 100 mL of dichloromethane. The solution was stirred for 1 h at room temperature. After evaporating off the solvent, the precipitate was washed with ethanol. Figure 1 shows the ^1H NMR spectrum of the (A) 4-ATP molecule and (B) the product in dichloromethane-d_2. The presence of various peaks corresponding to ATP moiety in Figure 1B shows the attachment of ATP to GNC. The line width of the peaks corresponding to ATP were broader in Figure 1B than those of 4-ATP molecule in solution (Figure 1A, confirming that 4-ATP molecules were really attached to the Au nanocluster surface.[72] The molar ratio of 4-ATP/C_6SH on the Au nanocluster were estimated using the integrated intensities of NMR peaks corresponding to NH_2 (3.5 ppm) and CH_3 (1.1 ppm) to be 50:14. It has been reported that 53 thiol molecules can adsorb on a GNC of the core size of 1.8 nm, which was used in this study.[72] Thus, 41 4-ATP molecules should be adsorbed on the GNC. TEM measurement showed that the core size of GNC was not changed during the place-exchange reaction.

Electrochemical Measurements. Electrochemical measurements were carried out in a three-compartment cell using a potentiostat/galvanostat (Hokuto Denko, HA-111) and a function generator (Hokuto Denko, HB-111). An ITO electrode was used as a working electrode after being washed with piranha solution (H_2SO_4/H_2O_2 = 3:1). A Pt wire and Ag/AgCl (saturated NaCl) were used as a counter electrode and reference electrode, respectively. The electrolyte solutions were deaerated by passing the ultrapure N_2 gas through them for more than 30 min before each measurement. Cyclic voltammograms (CVs) were recorded on an X-Y recorder (Graphtec, WX-1200).

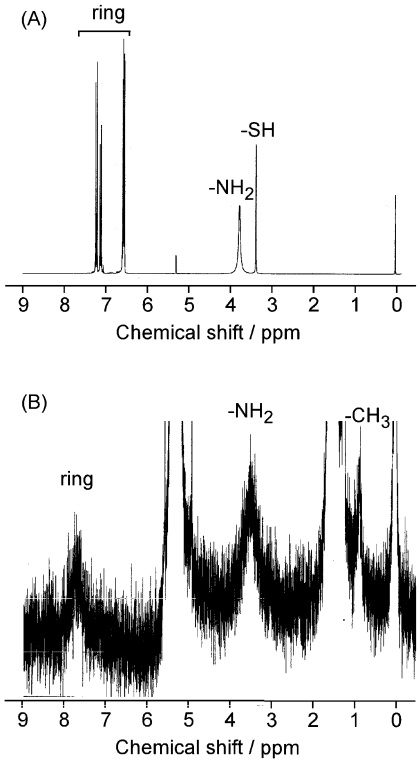

Figure 1. ^1H NMR spectra of (A) 4-ATP and (B) ATP-GNC in dichloromethane-d_2.

FT-IR Spectroscopy. FT-IRRAS measurements were carried out using a Bio-Rad FTS-30 equipped with a liquid-N_2-cooled HgCdTe detector. The light path in the spectrometer including the sample chamber was purged with dry air.

A thin-layer IR spectroelectrochemical cell with a CaF_2 window was used for in-situ electrochemical IR measurement.[73,74] The incidence angle of the infrared beam was approximately 65° and p-polarized light was used. A mirror-finish gold disk was used as a working electrode. It was pushed against the CaF_2 windows so that the liquid layer between the electrode and the windows became very thin to avoid the absorption of IR light in the solution layer. A total of 256 scans with 1 cm^{-1} resolution were collected at each potential. The measurements were carried out in 0.5 M $HClO_4$ aqueous solution. A solution was deaerated by passing ultrapure N_2 gas for more than 1 h before being injected in the cell. The spectrum obtained at 0 mV was used as a reference.

The substrate for ex-situ FT-IRRAS was vacuum-deposited gold prepared by vacuum evaporation of a 10-nm-thick Ti layer followed by vacuum evaporation of a 100-nm-thick Au layer onto glass. Ex-situ spectra were obtained by using a specular reflectance accessory (Pikes, PK-10), and the angle between a p-polarized IR probe beam and the substrate was set to be 10°. IR spectra were accumulated for 1024 scans.

X-ray Photoelectron Spectroscopy (XPS). XPS measurements were performed on a Rigaku XPS-7000 spectrometer using an Mg Kα X-ray source (1253.9 eV). The angle between the sample surface and the analyzer was fixed at 90° in all cases. After multilayers of 4-ATP and ATP-GNC had been prepared on the electrode by electrochemical polymerization, the electrode was removed from the electrochemical cell at 0 mV. In_{3d}, Sn_{3d}, Au_{4f}, N_{1s}, C_{1s}, and S_{2p} signals were acquired for 8, 8, 8, 256, 32, and 256 scans, respectively. All core levels were referenced

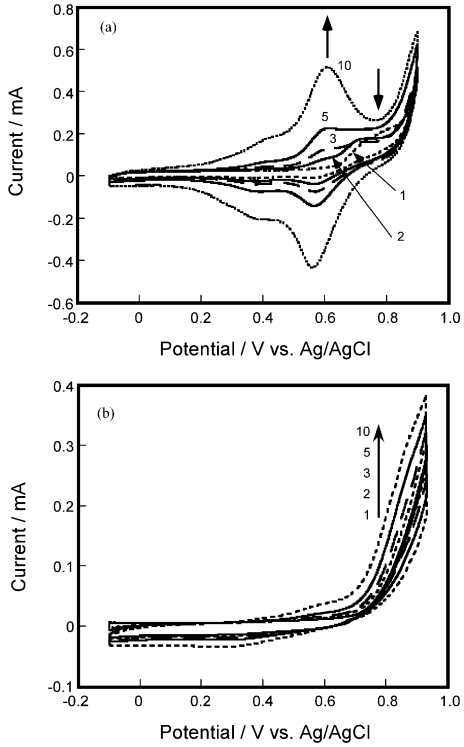

Figure 2. Cyclic voltammograms (CVs) of ITO electrodes in (A) 0.5 M $HClO_4$ containing 45 μg/mL ATP-GNC solution and (B) 0.5 M $HClO_4$ containing 0.17 mM 4-ATP solution. (WE: ITO, CE: Pt wire, and RE: Ag/AgCl, scan rate: 100 mV s^{-1}).

to $In_{3d5/2}$ (443.6 eV). ITO was used as a substrate for XPS measurements. Titanium (10-nm) followed by 100-nm Au were vacuum evaporated on the back and side of ITO to avoid charging.

In-Situ UV−Vis Spectroscopy. In-situ UV−visible measurements were performed in a 0.5 M $HClO_4$ solution using a UV−vis spectrometer (Hitachi, UV-3000). An ITO electrode was used as a working electrode. A Pt wire and Ag/AgCl (saturated NaCl) were used as the counter electrode and reference electrode, respectively. The electrolyte solution was deaerated by passing ultrapure N_2 gas for more than 30 min before each measurement.

Results

Electrochemical Behavior of an ITO Electrode in an ATP-GNC Solution. Figure 2 shows CVs of an ITO electrode obtained in (a) 0.5 M $HClO_4$ solution containing 45 μg/mL ATP-GNC and (b) 0.5 M $HClO_4$ solution containing 0.17 mM 4-ATP. In the ATP-GNC solution, an anodic peak was observed at 750 mV in the first cycle, but this peak disappeared after several potential cycles and a reversible redox peak at 550 mV and a shoulder at 400 mV were observed. These peaks grew as the number of potential cycles increased, suggesting the accumulation of electroactive species. Similar features were reported at an ATP-SAM modified Au electrode. In the case of an ATP-SAM modified Au electrode, an anodic peak was observed at 750 mV in the first cycle, but this peak disappeared after several potential cycles and a redox peak at 550 mV and a shoulder at 400 mV, which were due to oxidation of the surface polymerized layer, were observed, although these peaks did not grow because only a monolayer of ATP existed on the surface.

The electrochemical response of an ITO electrode in 0.5 M $HClO_4$ solution containing ATP was different from that of an ITO electrode in ATP-GNC solution and that of the ATP-SAM modified gold electrode as no clear peak was observed, and anodic current started to flow at 700 mV and increased monotonically as the potential became more positive.

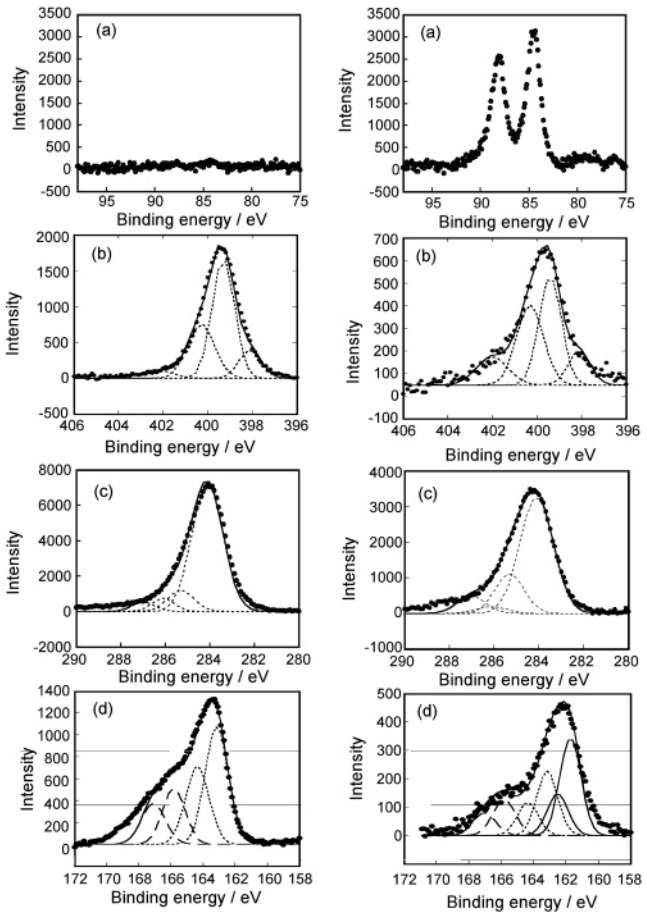

Figure 3. (a) Au_{4f}, (b) N_{1s}, (c) C_{1s}, and (d) S_{2p} XP spectra of an ITO electrode in 4-ATP (left side) and ATP-GNC (right side) solutions after electrochemical oxidation at 1 V for a total charge of 10 mC cm^{-2}.

XPS Spectra. Figure 3 shows XP spectra of an ITO electrode in (a) Au_{4f}, (b) N_{1s}, (c) C_{1s}, and (d) S_{2p} regions after electrochemical oxidation at 1 V for a total charge of 10 mC cm^{-2} in the 4-ATP solution (left panel) and ATP-GNC solution (right panel).

In Figure 3a, while no peaks were observed at the ITO electrode treated in the 4-ATP solution, peaks corresponding to $Au_{4f7/2}$ (84.4 eV) and $Au_{4f5/2}$ (88.0 eV) were clearly observed at the ITO electrode treated in the ATP-GNC solution, confirming the incorporation of gold nanoclusters in the film. Binding energies of Au_{4f} peaks of the GNC assembly are in good agreement with those reported for Au_{4f} of GNC covered with alkanethiol SAM on gold,[75,76] showing that 4-ATP molecules bound to the GNC surface by Au−S bonds.

XP spectra in the N_{1s} region of the ITO electrode treated in the ATP-GNC and 4-ATP solutions in Figure 3b showed essentially the same features with four peaks at 398.1, 399.3, 400.3, and 402 eV, which were observed in polyaniline in an emeraldine base state.[77,78] The peaks at 399.3 and 400.3 eV were assigned to a neutral amino group and positively charged amino group, respectively.[79] The peak at 398.1 eV was assigned to quinoide imine (−C═N−C−), and the peak at 402 eV was assigned to a positively charged amino group in the polyaniline film.[77,78]

XP spectra in the C_{1s} region of two samples in Figure 3c were essentially the same, with a peak at 284 eV corresponding

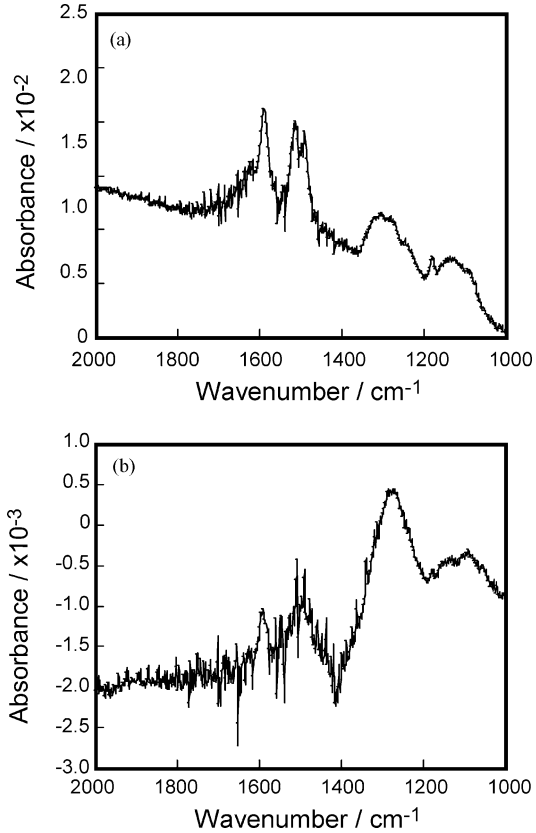

Figure 4. FT-IR spectra of gold electrodes modified with (a) ATP-GNC and (b) 4-ATP. The electrodes were removed from the electrochemical cell after being held at 0 mV for 5 min after electrochemical oxidation at 1 V for a total charge of 10 mC cm^{-2}.

to C═C and peaks at 285.3, 287, and 286.1 eV, which were assigned to the C−N bond, C−SO_3, and benzoquinone carbonyl (C═O), respectively.[79] The presence of a C═O peak in both cases suggests that the amine moiety in 4-ATP was changed to a quinone group by hydrolytic cleavage of the imine moiety.[79]

In addition to the two doublet peaks at 163.7 eV/165.8 eV and 164.9 eV/167.0 eV observed in the XP spectrum in the S_{2p} region of the ITO electrode treated in the ATP solution in Figure 3d, extra doublet peaks at 161.6 eV/162.8 eV were observed at the ITO electrode treated in the ATP-GNC solution. The peaks at 163.7 eV/164.9 eV were assigned to free thiol (−SH),[80−82] and those at 165.8 eV/167.0 eV were assigned to SO_3.[83,84] The doublet peaks at 161.6 eV/162.8 eV were assigned to thiolate bound to a gold atom (Au−S).[80−82] These results show that SO_3 and free thiol were present in both cases, but the Au−S bond existed only at an ITO modified in ATP-GNC solution. These results suggest that some of the 4-ATP molecules bound to the GNC surface through a Au−S bond and some remained unbound. The presence of a SO_3 moiety suggests that oxidation of the thiol moiety occurred in both cases.

Peak intensities of XPS in C_{1s}, N_{1s}, and S_{2p} of ATP assembly were larger than those of ATP-GNC assembly, although the total charges of electrochemical oxidation were the same. This is because GNC occupied a certain fraction of the modified layer in the latter.

Ex-Situ FT-IR Spectra. Figure 4 shows FT-IR spectra of gold electrodes after electrochemical oxidation at 1 V for a total charge of 10 mC cm^{-2} in 0.5 M $HClO_4$ solutions containing (a) ATP-GNC and (b) 4-ATP. The electrodes were removed from the electrochemical cell after being kept at 0 mV for 5 min after the electrochemical oxidation. Peaks at 1590, 1509, 1490, 1310, 1179, and 1136 cm^{-1} were observed at both ATP-GNC and 4-ATP assemblies. These peaks were also observed in polyaniline film and were assigned to C═C stretching of the benzene ring, N−B−N stretching (B meaning benzene type), N−H bending, C−N stretching in a polymer, a mode of N═Q═N (Q meaning quinone type), and a mode of Q═$^{+}$NH−B or B−NH−B.[77] These results suggest the formation of a polyaniline film on the electrode surface.

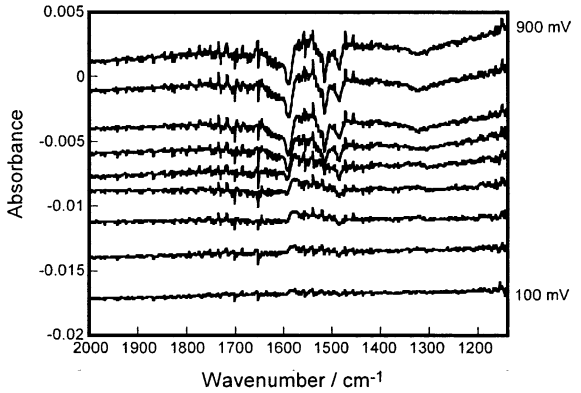

Figure 5. In-situ FT-IR spectra of gold electrode ATP-GNC assembly at various applied potentials. ATP-GNC assembly on the gold electrode was prepared by electrochemical oxidation at 1 V for a total charge of 10 mC cm^{-2} in a 0.5 M $HClO_4$ solution containing 45 μg/mL ATP-GNC.

In-Situ FT-IR Spectra. Figure 5 shows in-situ FT-IR spectra of an ATP-GNC modified gold electrode, which was prepared by electrochemical oxidation at 1 V for a total charge of 10 mC cm^{-2} in a 0.5 M $HClO_4$ solution containing 45 μg/mL ATP-GNC, measured in 0.5 M $HClO_4$ solution without ATP-GNC at various potentials with a reference spectrum obtained at 0 V. No clear peak was observed in the region of 1000−2000 cm^{-1} at 100 mV. When the potential was swept in the positive direction, negative-going bands at 1324, 1487, 1517, 1591, and 1609 cm^{-1} were observed. The peaks at 1487 and 1517 cm^{-1} were assigned to N−H bending and C−H bending, respectively. The band observed at 1591 cm^{-1} was assigned to a C═C stretching mode of the benzene ring.[85] The band observed at 1324 cm^{-1} was assigned to C−N stretching. The band at 1609 cm^{-1} corresponds to C═C stretching of the benzene ring.

In-Situ UV−Vis Spectra. Figure 6 shows absorption spectra of (a) ATP-GNC and (b) 4-ATP assemblies, which were prepared on ITO electrodes by electrochemical oxidation at 1 V for a total charge of 10 mC cm^{-2} in a 0.5 M $HClO_4$ solution containing 45 μg/mL ATP-GNC and in 0.5 M $HClO_4$ solution containing 0.17 mM 4-ATP, respectively, measured at −100 mV (solid line) and 900 mV (dotted line) in 0.5 M $HClO_4$. Three peaks at 315, 430, and 600 nm were observed in both cases and were assigned to π-π^* transition of the aromatic group, polaron absorption, and bipolaron absorption, respectively.[55,86,87] Absorbance in the region larger than 400 nm at 900 mV was greater than that at −100 mV in both cases. This corresponds to the increase of polaron and bipolaron in the oxidized state of polyaniline. The absorbance at 600 nm of the ATP-GNC modified ITO around 600 nm seemed to be greater than that of ITO modified with ATP, particularly in a reduced state.

Discussion

Mechanism of Electrochemical Assembly of ATP-GNC. Since electrochemical behavior for oxidation of ATP-GNC is similar to that of 4-ATP-SAM on a flat gold electrode as mentioned before (Figure 2(a)), the anodic peak at 750 mV

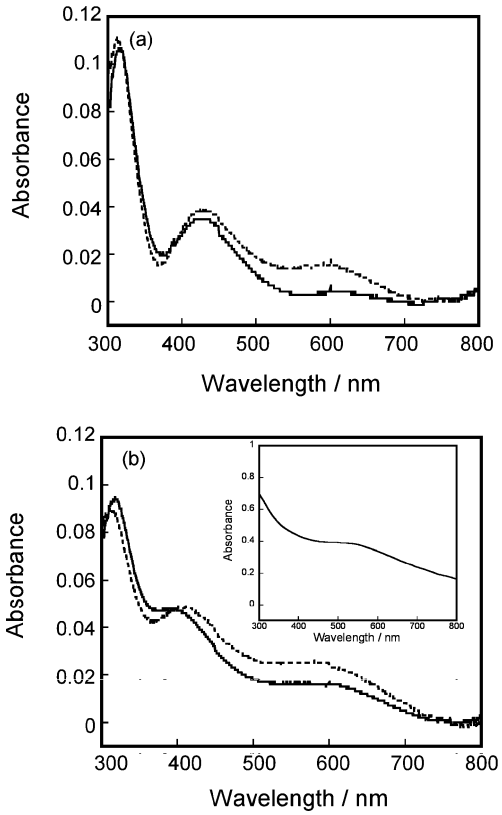

Figure 6. UV−vis spectra of (a) 4-ATP assembly and (b) ATP-GNC assembly measured at −100 mV (solid line) and 900 mV (dotted line). Both films on an ITO electrode were prepared by electrochemical oxidation at 1 V for a total charge of 10 mC cm^{-2}. Inset: UV−vis spectrum of ATP-GNC dispersed in CH_2Cl_2.

should correspond to the radical formation of a 4-ATP moiety as[79,88]

$$-NH_3^+ \rightarrow -NH_2^{+\bullet} + H^+ + e^- \qquad (2)$$

It was suggested that this radical cation was delocalization-stabilized on the gold surface in the case of a 4-ATP-SAM modified gold electrode. Similarly, this radical cation should be delocalization-stabilized on the GNC and react with a radical cation bound to another GNC, and a 4-ATP dimer, binding two GNCs, would be formed (Scheme 2).

The increase in the anodic peak at 550 mV with increase in potential cycles suggests successive electrochemical polymerization of ATP-GNC. The formation of a polyaniline layer with ATP-GNC on ITO was confirmed by XP spectra in the N_{1s} region, in which was observed a peak corresponding to quinoide imine (−C═N−C−).

Electrochemical Characteristics and Structure of ATP-GNC Assembly. It has been suggested that the redox peak at 550 mV corresponds to the following two-electron reaction within a polymerized ATP monolayer on gold.[79,85]

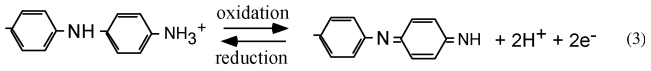

(3)

As a current peak at 550 mV was also observed and an IR peak due to C═N−C stretching was observed in the present study, this reaction also occurred in the ATP-GNC assembly. When the potential became more positive than 550 mV, the C−NH−C bond was expected to change to a C═N−C bond. In situ FT-IR measurement showed that the intensity of the C═C stretching mode of a benzene ring and C−N stretching decreased at 600 mV, confirming the conversion of a C−NH−C bond to a C═N−C bond.

SCHEME 2: Mechanism of Electrochemical Polymerization

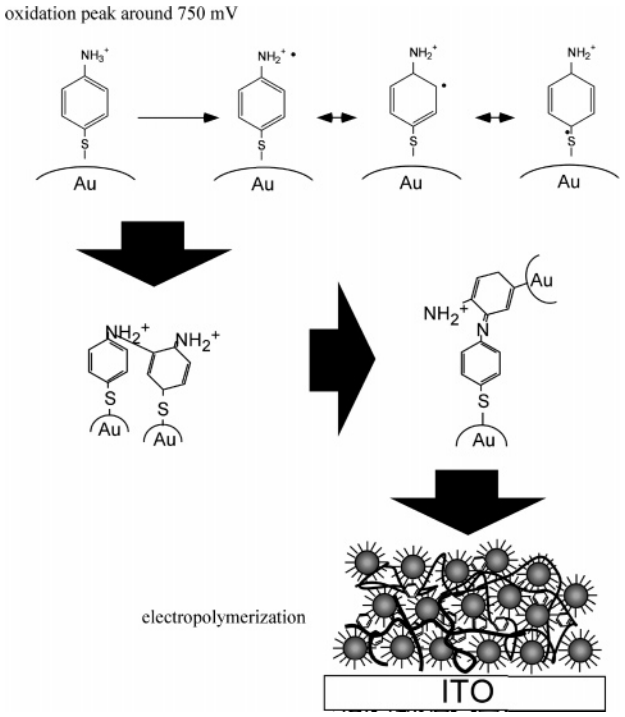

Although the formation of 4-ATP assembly on the ITO electrode was confirmed by XPS measurement, current response of 4-ATP assembly was different from that of ATP-GNC assembly, possibly due to low conductivity of ATP polymer without dispersed GNCs and/or difference in the electrochemical responses of polyaniline on ITO and GNC.

Sweep-rate dependence of the ATP-GNC modified ITO electrode, which was prepared by cycling the potential between 0 mV and 900 mV in a 0.5 M $HClO_4$ solution containing ATP-GNC, measured in 0.5 M $HClO_4$ by cycling the potential between 0 mV and 800 mV, is shown in Figure 7a. The shape of CVs did not change with the potential cycling between 0 mV and 800 mV, indicating that no further electrochemical polymerization took place in this potential region. The relation between scan rate and current density at 550 mV was linear, as shown in Figure 7b, confirming that electroactive species, that is, ATP-GNCs, were immobilized on a substrate by electrochemical polymerization.

The amount of ATP-GNC on the electrode was estimated from the charge of the anodic peak at 550 mV, that is, 0.125 mC cm^{-2}. The number of surface-attached ATP moieties was calculated to be 7.79×10^{14} cm^{-2}. Thus, the number of ATP-GNCs deposited on the surface should be 1.9×10^{13} cm^{-2} by considering the size of a GNC core, since the number of 4-ATP molecules adsorbed on each ATP-GNC is 41. The number of the thiol-covered GNCs per unit area with the closest packing was calculated to be $3.1-6.5 \times 10^{12}$ cm^{-2} by using the diameter of the thiol-covered GNC as 4.4−6.6 nm in this case. The experimentally observed number of ATP-GNCs per unit area was 4.5 times larger than the calculated value, suggesting 4−5 layers of ATP-GNC were deposited on the electrode.

At the polymerized ATP-SAM modified gold,[79,85] the shoulder at 400 mV was assigned to a redox reaction of the benzoquione moiety. The presence of a redox peak at 400 mV

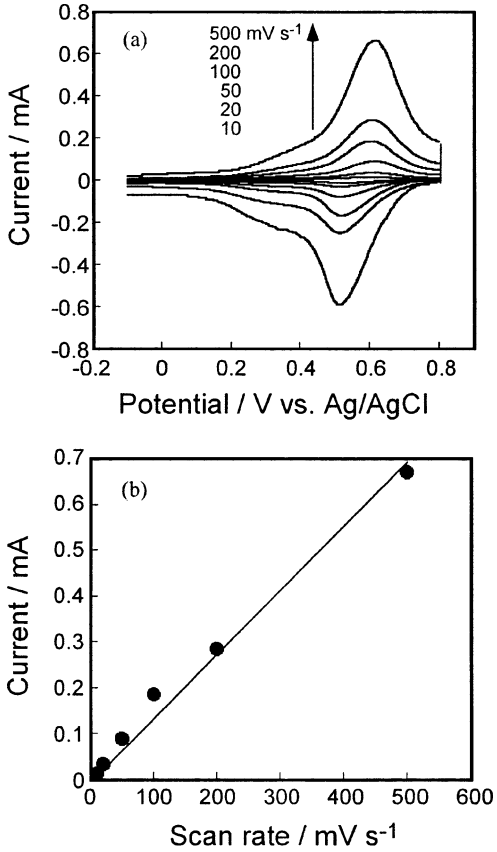

Figure 7. (a) CVs of an ITO electrode modified with ATP-GNC assembly in 0.5 M $HClO_4$ solution with various scan rates. (b) Relation between scan rate and current density of the oxidation peak at 550 mV.

in Figure 2a and a C_{1s} peak corresponding to C═O in XP spectra of ATP-GNC and ATP-modified ITO electrodes suggests the presence of a quinone moiety, formed by hydrolytic cleavage of an imine moiety,[79,85] in the ATP-GNC modified Au electrode. A fraction of 4-ATP molecules desorbed from the GNC surface and oxidation of the thiol moiety seemed to take place in both cases as S_{2p} XP spectra showed the presence of free −SH and $-SO_3$ groups.

The amount of the benzoquinone moiety depends on the pH of the reactant solution, and a small amount of benzoquinone moiety was produced in a solution of pH = 1.[85] Thus, the CV of ATP-GNC was different from that of a "typical" polyaniline film prepared in a solution of neutral pH, and a second oxidation−reduction peak of polyaniline film was observed only as a shoulder at 400 mV in ATP-GNC assembly.

Potential-Dependent Absorbance of ATP-GNC Assembly. Absorption spectra of ATP-GNC (Figure 6a) and ATP (Figure 6b)-modified ITO electrodes at −100 mV and 900 mV showed that the absorbance at 900 mV was greater than those at −100 mV in both cases and that the absorbance of the ATP-GNC modified electrode was greater than those of the ATP modified electrode at both potentials, particularly at −100 mV. The former result can be explained by the absorbance difference between a polyaniline film in an oxidized state and that of a polyaniline film in a reduced state, as mentioned before.[89] Plasmon absorption of ATP-GNC is weak, as shown in the inset of Figure 6b, and there is a possibility that the amount of ATP polymers deposited on the substrate is different from that of ATP-GNC assembly. Thus, to take into account the different amounts of ATP moiety in both cases, the absorbance was normalized using the 315 nm peak, then the difference spectra between the

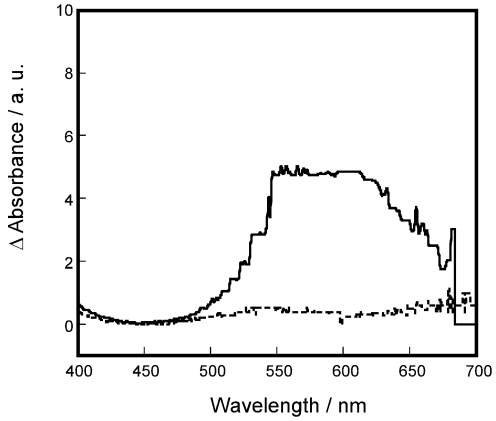

Figure 8. Difference absorption spectra of ATP-GNC assembly and ATP assembly (solid line: −100 mV, dotted line: 900 mV).

normalized spectra of ATP-GNC and ATP-modified electrodes at −100 mV and 900 mV were obtained by

$$\Delta Absorbance = \frac{Absorbance(ATP-GNCassembly) - Absorbance(ATPassembly)}{Absorbance(ATPassembly)} \quad (4)$$

and are shown in Figure 8. These spectra represent the absorbance of GNCs at each potential. At 900 mV, a rather broad peak was observed around 550−600 nm. The origin of this absorbance should be plasmon absorption. This peak was red-shifted compared with the plasmon absorption peak of ATP-GNC in solution, which was observed at around 520 nm, as shown in inset of Figure 6b. It is known that a red-shift of plasmon absorption is caused by aggregation of GNC.[90−92] Since ATP-GNC core was immobilized on the ITO surface through the polymerized aniline moiety, the distance between GNCs was expected to be short enough for GNCs to interact each other.[93]

Plasmon absorption at 900 mV was much smaller than that at −100 mV. This result is in good agreement with the results of a previous study on a multilayer of biferrocene-protected GNC.[14] They attributed this difference to the difference in the dielectric constant of the media around GNC caused by oxidation of the biferrocene group, that is, generation of a positive charge. It has been reported that the plasmon absorption peak is red-shifted and plasmon absorption intensity is decreased at positive potentials for other types of GNC assemblies.[94,95] Plasmon absorption peaks of alkanethiol-protected Au nanoclusters both in solution and multilayers have been known to be very broad.[9,72,94] Templeton et al. reported the effect of solvent refractive index and core charge on the surface plasmon absorbance of alkanethiol-protected Au nanoclusters and optical properties of GNC are changed by the applied potential.[96] In the present case, the state of polyaniline was changed from emeraldine base (reduced state) to emeraldine salt (oxidized state) at 550 mV as proved by in-situ FT-IR measurement. The refractive index of the polyaniline should therefore also change at this potential, as the refractive indexes (n) of emeraldine base and emeraldine salt were 1.56 and 1.13, respectively.[89] According to eq 1, plasmon absorption intensity is larger when the refractive index of the medium is higher. Furthermore, the increase of the electron density on the GNC may also contribute to the increase of absorption intensity at negative potentials.[94,95] Thus, plasmon absorption intensity is expected to be higher at a potential more negative than that in a redox peak at 550 mV. This is what was experimentally observed and it is confirmed

that intensity of plasmon absorption can be controlled by the applied potential.

Conclusions

4-ATP-modified GNC was assembled on Au and ITO substrates by electrochemical polymerization of the 4-ATP moiety on the GNC surface as proved by FT-IR and XPS measurements. Surface plasmon absorption of GNCs in the multilayer was potential-dependent. Plasmon absorption intensity was higher at potentials more positive than approximately 550 mV, although no shift of the peak position of plasmon absorption was observed, reflecting the lower dielectric constant of the media, that is, polyaniline, at a positive potential.

Acknowledgment. This work was partially supported by Grant-in-Aid for Scientific Research on Priority Areas "Molecular Nano Dynamics" from the Ministry of Education, Culture, Sports, Science and Technology (MEXT), Japan. We thank Prof. Shimazu for his help with the XPS measurement.

References and Notes

(1) Brust, M.; Walker, D.; Bethell, D.; Schiffrin, D. J.; Whyman, R. *J. Chem. Soc., Chem. Commun.* **1994**, 801.
(2) Freeman, R. G.; Grabar, K. C.; Allison, K. J.; Bright, R. M.; Davis, J. A.; Guthrie, A. P.; Hommer, M. B.; Jackson, M. A.; Smith, P. C.; Walter, D. G.; Natan, M. J. *Science* **1995**, *267*, 1629.
(3) Mirkin, C. A.; Letsinger, R. L.; Mucic, R. C.; Storhoff, J. J. *Nature* **1996**, *382*, 607.
(4) Reynolds, R. A., III; Mirkin, C. A.; Letsinger, R. L. *Pure. Appl. Chem.* **2000**, *72*, 229.
(5) Gittins, D. I.; Bethell, D.; Schiffrin, D. J.; Nichols, R. J. *Nature* **2000**, *408*, 67.
(6) Green, S. J.; Stokes, J. J.; Hostetler, M. J.; Pietron, J.; Murray, R. W. *J. Phys. Chem. B* **1997**, *101*, 2663.
(7) Chen, S. W.; Murray, R. W.; Feldberg, S. W. *J. Phys. Chem. B* **1998**, *102*, 9898.
(8) Hostetler, M. J.; Templeton, A. C.; Murray, R. W. *Langmuir* **1999**, *15*, 3782.
(9) Templeton, A. C.; Zamborini, F. P.; Wuelfing, W. P.; Murray, R. W. *Langmuir* **2000**, *16*, 6682.
(10) Zamborini, F. P.; Hicks, J. F.; Murray, R. W. *J. Am. Chem. Soc.* **2000**, *122*, 4514.
(11) Hicks, J. F.; Zamborini, F. P.; Osisek, A.; Murray, R. W. *J. Am. Chem. Soc.* **2001**, *123*, 7048.
(12) Wuelfing, W. P.; Murray, R. W. *J. Phys. Chem. B* **2002**, *106*, 3139.
(13) Wuelfing, W. P.; Green, S. J.; Pietron, J. J.; Cliffel, D. E.; Murray, R. W. *J. Am. Chem. Soc.* **2000**, *122*, 11465.
(14) Horikoshi, T.; Itoh, M.; Kurihara, M.; Kubo, K.; Nishihara, H. *J. Electroanal. Chem.* **1999**, *473*, 113.
(15) Men, Y.; Kubo, K.; Kurihara, M.; Nishihara, H. *Phys. Chem. Chem. Phys.* **2001**, *3*, 3427.
(16) Yamada, M.; Kubo, K.; Nishihara, H. *Chem. Lett.* **1999**, 1335.
(17) Yamada, M.; Tadera, T.; Kubo, K.; Nishihara, H. *Langmuir* **2001**, *17*, 2363.
(18) Ulman, A. *An Introduction to Ultrathin Organic Films from Langmuir−Blodgett to Self-Assembly*; Academic Press, San Diego, 1991.
(19) Finklea, H. O. In *Electroanalytical Chemstry*; Bird, A. J., Rubinstein, I., Eds.; Marcel Dekker: New York, 1996.
(20) Kondo, T.; Yanagida, M.; Nomura, S.; Ito, T.; Uosaki, K. *J. Electroanal. Chem.* **1997**, *438*, 121.
(21) Kondo, T.; Ito, T.; Nomura, S.; Uosaki, K. *Thin Solid Films* **1996**, *285*, 652.
(22) Kondo, T.; Yanagida, M.; Zhang, X. Q.; Uosaki, K. *Chem. Lett.* **2000**, 964.
(23) Kondo, T.; Kanai, T.; Iso-o, K.; Uosaki, K. *Z. Phys. Chem.* **1999**, *212*, 23.
(24) Uosaki, K.; Kondo, T.; Zhang, X. Q.; Yanagida, M. *J. Am. Chem. Soc.* **1997**, *119*, 8367.
(25) Kondo, T.; Horiuchi, S.; Yagi, I.; Ye, S.; Uosaki, K. *J. Am. Chem. Soc.* **1999**, *121*, 391.
(26) Yanagida, M.; Kanai, T.; Zhang, X. Q.; Kondo, T.; Uosaki, K. *Bull. Chem. Soc. Jpn.* **1998**, *71*, 2555.
(27) Kondo, T.; Kanai, T.; Uosaki, K. *Langmuir* **2001**, *17*, 6317.
(28) Ruppin, R. *Surf. Sci.* **1983**, *127*, 108.
(29) Aravind, P. K.; Metiu, H. *Surf. Sci.* **1983**, *124*, 506.
(30) Mayer, C.; Stich, N.; Palkovits, R.; Bauer, G.; Pittner, F.; Schalkhammer, T. *J. Pharm. Biomed. Anal.* **2001**, *24*, 773.
(31) Mayer, C.; Palkovits, R.; Bauer, G.; Schalkhammer, T. *J. Nanoparticle Res.* **2001**, *3*, 361.
(32) Mie, G. *Ann. Phys.* **1908**, *25*, 377.
(33) Kreibig, U.; Vollmer, M. *Optical Properties of Metal Clusters*; Springer: Berlin, 1995.
(34) Henglein, A. *J. Phys. Chem.* **1993**, *97*, 5457.
(35) Nakanishi, T.; Ohtani, B.; Shimazu, K.; Uosaki, K. *Chem. Phys. Lett.* **1997**, *278*, 233.
(36) Nakanishi, T.; Ohtani, B.; Uosaki, K. *J. Electroanal. Chem.* **1998**, *455*, 229.
(37) Nakanishi, T.; Ohtani, B.; Uosaki, K. *J. Phys. Chem. B* **1998**, *102*, 1571.
(38) Nakanishi, T.; Ohtani, B.; Uosaki, K. *Jpn. J. Appl. Phys.* **1999**, *38*, 518.
(39) Hu, K.; Brust, M.; Bard, A. J. *Chem. Mater.* **1998**, *10*, 1160.
(40) Gittins, D. I.; Bethell, D.; Nichols, R. J.; Schiffrin, D. J. *Adv. Mater.* **1999**, *11*, 737.
(41) Brust, M.; Bethell, D.; Kiely, C. J.; Schiffrin, D. J. *Langmuir* **1998**, *14*, 5425.
(42) Kondo, T.; Okamura, M.; Uosaki, K. *Chem. Lett.* **2001**, 930.
(43) Uosaki, K.; Kondo, T.; Okamura, M.; Song, W. *Faraday Discuss.* **2002**, *121*, 373.
(44) Song, W.; Okamura, M.; Kondo, T.; Uosaki, K. *J. Electroanal. Chem.* **2003**, *554−555*, 385.
(45) Song, W.; Okamura, M.; Kondo, T.; Uosaki, K. *Phys. Chem. Chem. Phys.* **2003**, *5*, 5279.
(46) Uosaki, K.; Okamura, M.; Ebina, K. *Faraday Discuss.* **2004**, *125*, 39.
(47) Pardo-Yissar, V.; Gabai, R.; Shipway, A. N.; Bourenko, T.; Willner, I. *Adv. Mater.* **2001**, *13*, 1320.
(48) Pardo-Yissar, V.; Katz, E.; Lioubashevski, O.; Willner, I. *Langmuir* **2001**, *17*, 1110.
(49) Torimoto, T.; Tsumura, N.; Miyake, M.; Nishizawa, M.; Sakata, T.; Mori, H.; Yoneyama, H. *Langmuir* **1999**, *15*, 1853.
(50) Torimoto, T.; Kontani, H.; Sakata, T.; Mori, H.; Yoneyama, H. *Chem. Lett.* **1999**, 379.
(51) Torimoto, T.; Tsumura, N.; Nakamura, H.; Kuwabata, S.; Sakata, T.; Mori, H.; Yoneyama, H. *Electrochim. Acta* **2000**, *45*, 3269.
(52) Quiros, I.; Yamada, M.; Kubo, K.; Mizutani, J.; Kurihara, M.; Nishihara, H. *Langmuir* **2002**, *18*, 1413.
(53) Yamada, M.; Quiros, I.; Mizutani, J.; Kubo, K.; Nishihara, H. *Phys. Chem. Chem. Phys.* **2001**, *3*, 3377.
(54) Yamada, M.; Nishihara, H. *Chem. Commun.* **2002**, 2578.
(55) Kobayashi, T.; Yoneyama, H.; Tamura, H. *J. Electroanal. Chem.* **1984**, *161*, 419.
(56) MacDiarmid, A. G.; Epstein, A. J. *Faraday Discuss. Chem. Soc.* **1989**, *88*, 317.
(57) Krutovertsev, S. A.; Ivanova, O. M.; Sorokin, S. I. *J. Anal. Chem.* **2001**, *56*, 1057.
(58) Hosseini, S. H.; Entezami, A. A. *Polym. Adv. Technol.* **2001**, *12*, 524.
(59) Kang, X. F.; Cheng, G. J.; Dong, S. J. *Electrochem. Commun.* **2001**, *3*, 489.
(60) Eftekhari, A. *Sens. Actuators, B−Chem.* **2001**, *80*, 283.
(61) Cooper, J. C.; Haemmerle, M.; Schuhmann, W.; Schmidt, H. L. *Biosens. Bioelectron.* **1993**, *8*, 65.
(62) Goto, F.; Abe, K.; Okabayashi, K.; Yoshida, T.; Morimoto, H. *J. Power Sources* **1987**, *20*, 243.
(63) Kitani, A.; Kaya, M.; Sasaki, K. *J. Electrochem. Soc.* **1986**, *133*, 1069.
(64) Taguchi, S.; Tanaka, T. *J. Power Sources* **1987**, *20*, 249.
(65) Boschi, T.; Di Vona, M. L.; Tagliatesta, P.; Pistoia, G. *J. Power Sources* **1988**, *24*, 185.
(66) Sarkar, S.; Basumallick, I. N. *J. Electrochem. Soc. India* **1988**, *37*, 63.
(67) Genies, E. M.; Hany, P.; Santier, C. *J. Appl. Electrochem.* **1988**, *18*, 751.
(68) Wang, B.; Li, G.; Li, C.; Wang, F. *J. Power Sources* **1988**, *24*, 115.
(69) Osaka, T.; Ogano, S.; Naoi, K.; Oyama, N. *J. Electrochem. Soc.* **1989**, *136*, 306.
(70) Paul, E. W.; Ricco, A. J.; Wrighton, M. S. *J. Phys. Chem.* **1985**, *89*, 1441.
(71) Hatchett, D. W.; Josowicz, M.; Janata, J.; Baer, D. R. *Chem. Mater.* **1999**, *11*, 2989.
(72) Hostetler, M. J.; Wingate, J. E.; Zhong, C. J.; Harris, J. E.; Vachet, R. W.; Clark, M. R.; Londono, J. D.; Green, S. J.; Stokes, J. J.; Wignall, G. D.; Glish, G. L.; Porter, M. D.; Evans, N. D.; Murray, R. W. *Langmuir* **1998**, *14*, 17.
(73) Shimazu, K.; Ye, S.; Sato, Y.; Uosaki, K. *J. Electroanal. Chem.* **1994**, *375*, 409.

(74) Ye, S.; Akutagawa, H.; Uosaki, K.; Sasaki, Y. *Inorg. Chem.* **1995**, *34*, 4527.
(75) Johnson, S. R.; Evans, S. D.; Mahon, S. W.; Ulman, A. *Langmuir* **1997**, *13*, 51.
(76) Kondo, T.; Yanagida, M.; Shimazu, K.; Uosaki, K. *Langmuir* **1998**, *14*, 5656.
(77) Tan, K. L.; Tan, B. T. G.; Kang, E. T.; Neoh, K. G. *J. Chem. Phys.* **1991**, *94*, 5382.
(78) Kang, E. T.; Neoh, K. G.; Tan, K. L. *Prog. Polym. Sci.* **1998**, *23*, 277.
(79) Lukkari, J.; Kleemola, K.; Meretoja, M.; Ollonqvist, T.; Kankare, J. *Langmuir* **1998**, *14*, 1705.
(80) Castner, D. G.; Hinds, K.; Grainger, D. W. *Langmuir* **1996**, *12*, 5083.
(81) Laibinis, P. E.; Whitesides, G. M.; Allara, D. L.; Tao, Y. T.; Parikh, A. N.; Nuzzo, R. G. *J. Am. Chem. Soc.* **1991**, *113*, 7152.
(82) Sato, Y.; Ye, S.; Haba, T.; Uosaki, K. *Langmuir* **1996**, *12*, 2726.
(83) Evans, S. D.; Goppert-Berarducci, K. E.; Urankar, E.; Gerenser, L. J.; Ulman, A. *Langmuir* **1991**, *7*, 2700.
(84) Ishida, T.; Choi, N.; Mizutani, W.; Tokumoto, H.; Kojima, I.; Azehara, H.; Hokari, H.; Akiba, U.; Fujihira, M. *Langmuir* **1999**, *15*, 6799.
(85) Raj, C. R.; Kitamura, F.; Ohsaka, T. *Langmuir* **2001**, *17*, 7378.
(86) Maciel, G. S.; Bezerra, A. G.; Rakov, N.; de Araujo, C. B.; Gomes, A. S. L.; de Azevedo, W. M. *J. Opt. Soc. Am. B* **2001**, *18*, 1099.
(87) Brandl, V.; Holze, R. *Ber. Bunsen-Ges. Phys. Chem.* **1997**, *101*, 251.
(88) Hayes, W. A.; Shannon, C. *Langmuir* **1996**, *12*, 3688.
(89) Greef, R.; Kalaji, M.; Peter, L. M. *Faraday Discuss. Chem. Soc.* **1989**, *88*, 277.
(90) Lahav, M.; Gabriel, T.; Shipway, A. N.; Willner, I. *J. Am. Chem. Soc.* **1999**, *121*, 258.
(91) Shipway, A. N.; Lahav, M.; Blonder, R.; Willner, I. *Chem. Mater.* **1999**, *11*, 13.
(92) Grabar, K. C.; Freeman, R. G.; Hommer, M. B.; Natan, M. J. *Anal. Chem.* **1995**, *67*, 735.
(93) Shipway, A. N.; Lahav, M.; Gabai, R.; Willner, I. *Langmuir* **2000**, *16*, 8789.
(94) Yamada, M.; Nishihara, H. *Chemphyschem* **2004**, *5*, 555.
(95) Toyota, A.; Nakashima, N.; Sagara, T. *J. Electroanal. Chem.* **2004**, *565*, 335.
(96) Templeton, A. C.; Pietron, J. J.; Murray, R. W.; Mulvaney, P. *J. Phys. Chem. B* **2000**, *104*, 564.